frontiers | Frontiers in Materials

TYPE Original Research
PUBLISHED 24 March 2023
DOI 10.3389/fmats.2023.1141154

OPEN ACCESS

EDITED BY
Chengchen Guo,
Westlake University, China

REVIEWED BY
Xin Yu,
Westlake University, China
Sanjana Gopalakrishnan,
Tufts University, United States

*CORRESPONDENCE
Jin Yoo,
jyoo@kist.re.kr

SPECIALTY SECTION
This article was submitted to Biomaterials and Bio-Inspired Materials, a section of the journal Frontiers in Materials

RECEIVED 10 January 2023
ACCEPTED 13 March 2023
PUBLISHED 24 March 2023

CITATION
Roh S, Lee K, Jung Y and Yoo J (2023), Facile method for immobilization of protein on elastic nanofibrous polymer membranes.
Front. Mater. 10:1141154.
doi: 10.3389/fmats.2023.1141154

Facile method for immobilization of protein on elastic nanofibrous polymer membranes

Soonjong Roh[1,2], Kangwon Lee[2,3], Youngmee Jung[2,4] and Jin Yoo[1]*

[1]Center for Biomaterials, Biomedical Research Institute, Korea Institute of Science and Technology (KIST), Seoul, South Korea, [2]Department of Applied Bioengineering, Graduate School of Convergence Science and Technology, Seoul National University, Seoul, South Korea, [3]Research Institute for Convergence Science, Seoul National University, Seoul, South Korea, [4]School of Electrical and Electronic Engineering, YU-KIST Institute, Yonsei University, Seoul, South Korea

Surface modification of polymeric scaffolds for biomedical applications is a versatile and widely used method to improve interactions between scaffolds and cells. Specifically, chemical immobilization of proteins to polymeric scaffolds provides significant advantages such as stable and biocompatible properties, however, it generally requires expensive instruments or complex steps. In this study, the facile method is presented that changes poly (l-lactide-co-caprolactone) electrospun nanofibrous membranes to be cell-friendly and bioactive by chemical immobilization of proteins onto membranes. The model protein, bovine serum albumin was bound onto the nanofibrous membranes *via* aminolysis and subsequent covalent grafting. The surface modification effects of the nanofibrous membranes including surface morphologies, mechanical properties, and wettability were investigated. In addition, *in vitro* studies have demonstrated that adhesion and proliferation of human dermal fibroblasts are promoted in protein-immobilized membranes compared to bare nanofibrous membranes.

KEYWORDS

protein immobilization, electrospinning, nanofibers, Poly(l-lactic-co-ε-caprolactone), surface modifcation

1 Introduction

Variation in material surface properties has attracted attention in biomaterial science since the interactions between scaffolds and cells are crucial factor in biological activity. Primary surface properties of biomaterials include roughness, topography, chemical functional groups, balance between hydrophilicity and hydrophobicity, and surface free energy, etc (Ma et al., 2007; Lin et al., 2018; Jeznach et al., 2019). Surface modification has a great advantage in the modulating material surfaces without altering bulk properties since cell-material interactions are mainly related to interfaces. In particular, surface functionalization of biomaterials by biomolecule immobilization has been spotlighted in biomedical fields including cell-interactive scaffolds and biosensors.

Among diverse biomaterials (e.g., metals, ceramics, polymers, etc.), polymers are the most widely used for biomedical applications due to their biocompatible nature and relatively inexpensive cost when compared to metals and ceramics (Teo et al., 2016; Morelli and Hawker, 2021). To obtain stable functionalized polymer surfaces by biomolecules, specifically covalently conjugated surfaces, the commonly used methods

are plasma treatment (Morelli and Hawker, 2021), electron-beam process (Schmidt et al., 2021), layer-by-layer technique (Amin Yavari et al., 2020), and surface grafting polymerization (Oktay et al., 2015). However, it generally requires expensive instruments or complex steps. Therefore, wet chemistry such as hydrolysis and aminolysis has often been adopted for surface modification of polymeric surfaces due to their simple process (Jeznach et al., 2022). Additionally, EDC/NHS coupling chemistry is widely used in surface modifications to immobilize biomolecule proteins onto the functionalized polymer surfaces (Psarra et al., 2017). EDC, coupled with NHS, facilitates the formation of amide bonds between carboxyl and amine groups, which enables the immobilization of proteins on the surface. Furthermore, EDC is known to improve the stability and mechanical strength of biomaterials by acting as a cross-linker between biomolecules (Powell and Boyce, 2006).

Contrary to metals and ceramics, polymers can be easily fabricated into a wide range of architectures such as films, 3D scaffolds, meshes, and so on (Chung et al., 2021). In particular, nanofibrous membranes are considered promising biomaterials by mimicking the extracellular matrix (Masaeli et al., 2017; Yan et al., 2022). Various methods have been used for the fabrication of nanofibrous scaffolds, including self-assembly, phase separation, electrospinning (Yao et al., 2020). Among these techniques, electrospinning stands out due to its well-established and easy control over fiber diameter, as well as wide range of biomaterials that can be used. While imitating the complex fibrous structure of the native ECM can be challenging, electrospinning enables the fabrication of biomimetic fibrous scaffolds at the micron and sub-micron scale (Keshvardoostchokami et al., 2021). Furthermore, electrospun nanofibers act as excellent substrates for immobilization due to their large surface area to volume ratio and interconnectivity (Smith et al., 2020). While biomolecules can be immobilized by physical adsorption, covalent conjugation offers a method of permanently anchoring the active material to the fibrous surface, providing high efficiency, good specificity, and excellent stability.

Herein, we utilized poly (l-lactide-co-caprolactone) (PLCL) electrospun nanofibrous membranes as substrates and induced protein immobilization *via* aminolysis and EDC/NHS chemistry. Although PLCL has biocompatible and elastic properties that act as a great advantage in biomedical applications, hydrophobic properties and the absence of bioactive sites hamper cell adhesion, as reported in previous studies (Yoo et al., 2020; Yoo et al., 2021). Therefore, we have demonstrated that introducing bovine serum albumin (BSA) into PLCL electrospun membranes through a facile post-modification method led to increasing human dermal fibroblasts (HDFs) adhesion and proliferation, proving successful functionalization of the membranes. Furthermore, characterization of the modified membranes such as surface morphologies, mechanical properties, and wettability was performed. As the aminolysis treatment time increased, the amount of BSA immobilization increased, whereas the mechanical stability is decreased. Conclusively, the surface treatment conditions should vary depending on whether high mechanical properties are required or bioactivity is preferred, that is, depending on the application field.

2 Experimental section

2.1 Materials

In order to synthesize and fabricate PLCL fibrous membranes, L-lactide (LA) and ε-caprolactone (CL), and 1,1,1,3,3,3-Hexafluoro-2-propanol (HFIP, > 99%) were purchased from Purac Biochem (Gorinchem, Netherlands), Sigma Aldrich (St. Louis, MO, United States), and TCI (Tokyo, Janpan) respectively. For aminolysis, Ethylenediamine (ReagentPlus®, > 99%), Ninhydrin, and Isopropyl alcohol (> 99.5%) were purchased from Sigma Aldrich (St. Louis, MO, United States) and Daejung (Korea), respectively. Bovine Serum Albumin (BSA), Albumin–fluorescein isothiocyanate conjugate (FITC-BSA), and 1-Ethyl-3-(3-dimethylaminopropyl)-carbodiimide (EDC) were purchased from Sigma Aldrich (St. Louis, MO, United States), and N-hyroxysuccinimide (NHS) was obtained from Thermo Fisher (Waltham, MA, United States). Dulbecco's Modified Eagle Medium (DMEM), Fetal Bovine Serum (FBS), Penicillin-Streptomycin, and Dulbecco's Phosphate Buffered Saline (DPBS, 1X) were all purchased from Gibco (St. Louis, MO, United States) and 0.25% Trypsin was from Corning Inc. (NY, United States).

2.2 Elastic nanofibrous membrane preparation

PLCL (LA/CL = 50:50) was synthesized as previously reported (Jeong et al., 2004; Kim et al., 2019). Briefly, LA, CL, 1-dodecanol (initiator), and tin (II) 2-ethylhexanoate (catalyst) with the molar ratio of 10,000:10,000:1:1 were put in the round flask and polymerization was conducted at 150°C for 24 h under vacuum. The molecular weight distribution of the synthesized PLCL was analyzed using GPC (gel permeation chromatography, 1,260 Infinity II, Agilent). The synthesized PLCL was then dissolved in HFIP at 10% w/v concentration. The PLCL solution was filled in a 10 mL syringe with a stainless needle (21G) and electrospun at a voltage of 21 kV with a high-voltage power supply (NanoNC, Korea). The distance between the needle and drum collector was 15 cm and the feed rate of the syringe pump was 0.4 mL/h. The electrospun PLCL was collected on the rotating drum collector at a speed of 200 rpm.

2.3 Aminolysis of PLCL electrospun membranes

For aminolysis treatment of the surface, the PLCL fiber was immersed in 6% w/v ethylenediamine in isopropyl alcohol at 37°C for 5 and 15 min with shaking at 100 rpm, respectively. Based on previous studies, the aminolysis treatment time was set to a mild condition, ensuring that the membrane would not degrade (Jeznach et al., 2022). After the reaction, the fiber was rinsed three times with deionized (DI) water and dried in a vacuum overnight. The obtained PLCL fibrous membranes were used for characterization and followed by BSA immobilization.

TABLE 1 Experimental groups of the bare, aminolyzed, and protein-grafted PLCL membranes.

Group	Surface Modification			
	Scaffold type	Aminolysis time (min)	Ethylenediamine conc. (w/v)	BSA conc. (μg/ml)
PLCL	PLCL nanofiber	–	–	–
5A	PLCL nanofiber	5	6%	–
15A	PLCL nanofiber	15	6%	–
5A_BSA	PLCL nanofiber	5	6%	200
15A_BSA	PLCL nanofiber	15	6%	200

2.4 Immobilization of protein on PLCL membranes

To improve cell-surface affinity, BSA and RGD immobilization on the aminolyzed PLCL fiber was performed. The proteins were grafted onto the PLCL fibrous membranes through EDC/NHS coupling chemistry. First, 20 mM of EDC and 50 mM of NHS were prepared in 0.1 M MES buffer. Then, BSA and RGD were respectively dissolved in the above solution at the same concentration of 200 μg/mL. Finally, the surface-modified fiber was immersed in the BSA or RGD solution overnight at room temperature, sufficiently washed with DI water, and dried in a vacuum. The prepared samples were named as follows: PLCL, 5 A, 15 A, 5A_BSA, 15A_BSA (Table 1).

2.5 Physicochemical characterization of the modified membranes

2.5.1 Surface analysis

To observe the morphological properties and identify the elemental composition of the surface-modified PLCL membranes, scanning electron microscopy (SEM) with energy-dispersive spectroscopy (EDS) (Inspect F50, FEI company, Hillsboro, OR, United States) was used. Before the analysis, all samples were coated with Pt using a sputter coater. The images were acquired at an accelerating voltage was 5 kV to minimize the deformation of samples by high voltage. Exceptionally, EDS analysis was conducted at an accelerating voltage of 15 kV to enhance the electron beam penetration into the surfaces. The fiber diameter distribution was analyzed using Image J (Version 1.53v 21 November 2022, National Institutes of Health, Bethesda, MD, United States). The surface topography was evaluated using an atomic force microscopy (AFM) (XE-100, Park Systems, Korea) in non-contact mode and data was processed by Gwddion. The confirmation of BSA covalent conjugation with the aminolyzed PLCL membrane was evaluated by X-ray photon spectroscopy (XPS) and attenuated total reflection-Fourier transform infrared (ATR-FTIR). The XPS measurements were performed on PLCL, 5A_BSA, and 15A_BSA, using an XPS instrument (Nexsa, ThermoScientific., MA) equipped with monochromated AI Kα (1,486.6 eV) radiation. All XPS spectra were obtained in the constant analyzer energy (CAE) mode with a 400 μm spot size, and the charging correction was carried out based on adventitious carbon (284.8 eV). In addition, molecular structure and bonding information of the bare and BSA-grafted membranes were obtained by ATR-FTIR (Nicolet iS20, ThermoScientific., MA) in the absorbance mode from 400 to 4,000 cm^{-1}.

2.5.2 Mechanical testing

The tensile properties including Young's modulus, stress at break, and strain at break were evaluated using an Instron (Model 5,966, Instron Corp., Norwood, MA, United States). For the measurement, we prepared each sample with a size of 9 mm (width) x 5 mm (length). The tensile testing was conducted at a 50 mm/min crosshead speed using a 1 kN load cell. The average thicknesses of the PLCL membranes were determined by a thickness gauge (Mitutoyo, Japan) and all samples were measured in dry at room temperature.

2.5.3 Ninhydrin assay

To detect and quantify amino groups on the surface of the PLCL membranes, a ninhydrin colorimetric assay was performed. Firstly, to visualize the amino groups on the surfaces, 0.2% w/v of ninhydrin solution was beforehand prepared by dissolving ninhydrin powder in 100% ethanol and the membranes were placed on a slide glass. The ninhydrin solution was dropped onto each sample to be fully wetted and the samples were incubated for 15 min at 37°C. For quantification of the amino groups, 2% w/v of ninhydrin solution was used. The membranes of the same size were separately put into glass vials and 0.5 mL of the ninhydrin solution was added to each vial. After heating the vials for 10 min at 100°C using a hot plate, 1 mL of isopropyl alcohol per vial was added. Finally, the absorbance of the samples was measured at 570 nm with a microplate reader (VersaMAX, Molecular Devices, United States). The absorbance was calculated based on the standard curve with known concentrations of ethylenediamine in isopropyl alcohol.

2.5.4 FITC-BSA analysis

To evaluate the function of amino groups on the surfaces, FITC-BSA was immobilized on the aminolyzed membrane surfaces. Firstly, FITC-BSA was dissolved in PBS (pH 7.4) at a concentration of 200 μg/mL. The PLCL membranes of the same size were placed into the 24-well cell culture plate and 300 μL of FITC-BSA solution was added to each well. After incubation for 90 min at 37°C, the fluorescent images were observed by fluorescent microscopy (Eclipse Ts2R, Nikon, Japan) and the intensity of fluorescence was quantified with ImageJ. The quantification of

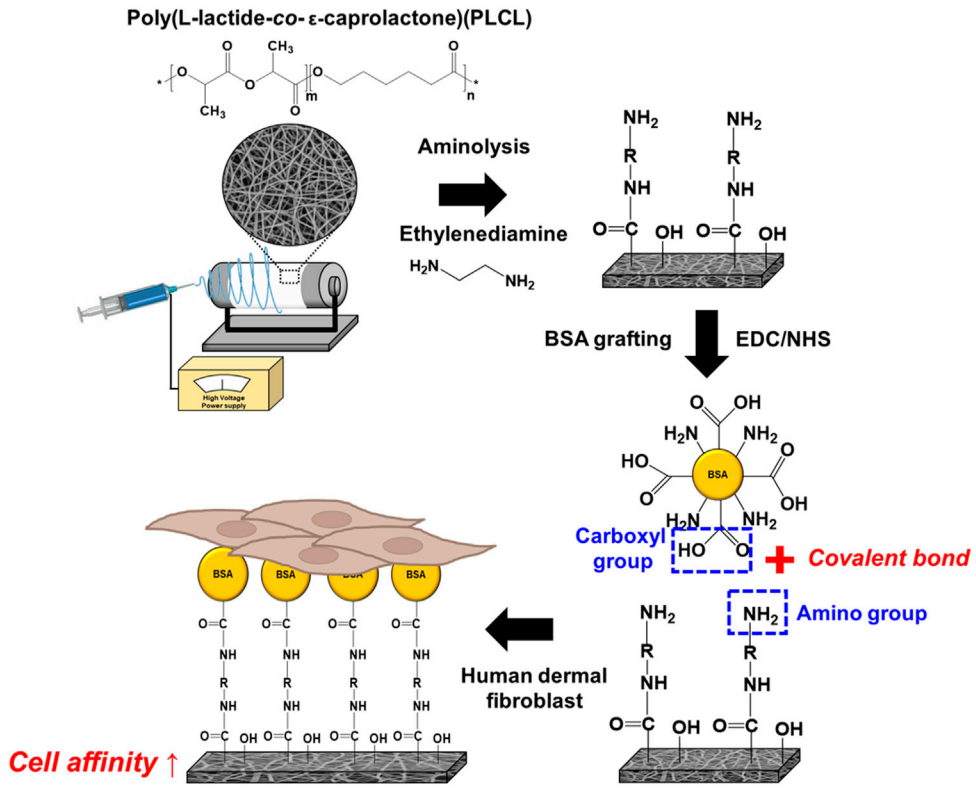

FIGURE 1
A schematic diagram of the fabrication and surface modification of the elastic nanofibrous PLCL membrane.

BSA grafted on the surfaces was also evaluated using FITC-BSA. We grafted FITC-BSA on the aminolyzed membranes with EDC/NHS coupling agent in the dark overnight at three different concentrations of 20, 200, and 2000 μg/mL. The analysis was performed as abovementioned with ImageJ.

2.5.5 Water contact angle

The wettability of the samples was determined by the water contact angle. The water contact angle (WCA) was measured using a droplet analyzer (SmartDrop, Femtobiomed, Korea). For the accuracy of the experiment, all samples were rinsed with DI water and fully dried before the measurement. The measurement was repeated three times and the mean value with standard deviation was recorded as result.

2.6 Cell-PLCL membrane interaction

2.6.1 Cell culture

Human dermal fibroblasts (HDFs) were used for evaluating the biocompatibility of the PLCL membranes. The HDFs were grown in Dulbecco's modified Eagle's medium supplemented with 10% v/v fetal bovine serum and 100 units mL^{-1} of penicillin-streptomycin. The cells were cultured in a humidified atmosphere of 5% CO_2 at 37°C, and the culture medium were refreshed every 2–3 days.

2.6.2 Cell proliferation assay

To determine the cell proliferation on the surface-modified membranes, the cell counting kit-8 (CCK-8, Dojindo Molecular Technologies, Rockville, MD, United States) was used, which measures reduced tetrazolium salt into a soluble colored formazan product by living cells. Before the cell seeding, all membranes were sterilized using 70% ethanol for 30 min and washed with DPBS several times. 5,000 cells cm^{-1} were seeded onto each membrane and placed onto a 48-well cell culture plate (Thermo Fisher, Waltham, MA, United States) and cultured for 1, 3, and 5 days.

2.6.3 Cell adhesion on the PLCL membranes

To observe the morphologies of the cells on the PLCL membranes over incubation time, immunofluorescence staining was performed. The PLCL membranes seeded with the cells were fixed with 4% paraformaldehyde (Biosesang, Gyeonggido, Korea) for 30 min at room temperature and washed with DPBS. The fixed cells were then permeabilized in 0.1% Triton-X 100 (Biosesang, Gyeonggido, Korea) in DPBS for 5 min and blocked with 1% BSA in DPBS for 30 min. Filamentous actin (F-action) of the cells was firstly stained with Alexa Fluor™ 594 Phalloidin (1:400, Thermo Fisher, Waltham, MA, United States), followed by the nucleus stained with 4′-6-diamidino-2-phenylindole (DAPI, 1:000, Molecular Probes, United States). Finally, fluorescent images were observed using fluorescent microscopy (Eclipse Ts2R, Nikon, Japan).

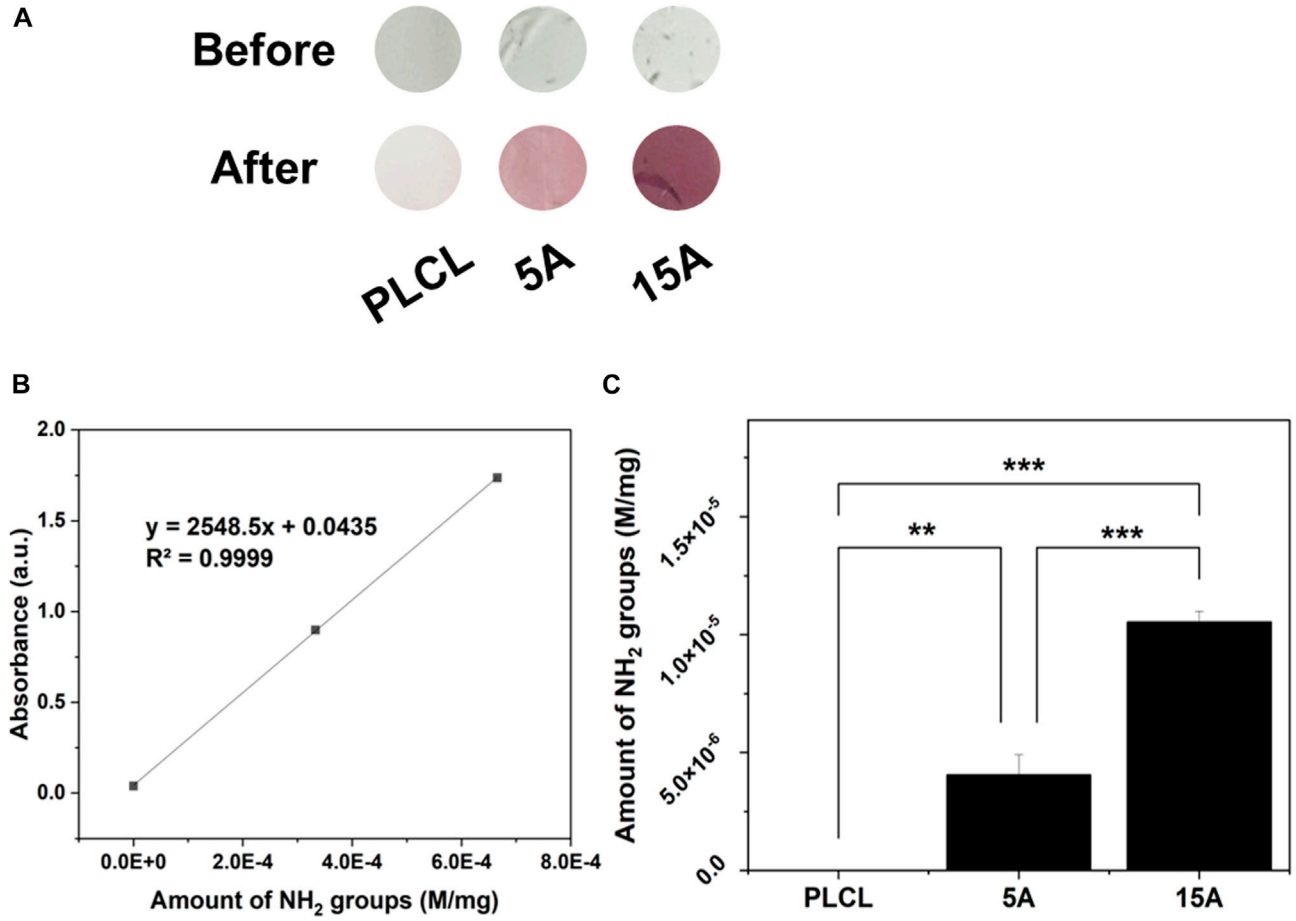

FIGURE 2
The viualization and quantification of the amino groups grafted on the amnolyzed PLCL electrospun membranes. **(A)** The PLCL membrane images after ninhydrin staining. **(B)** The standard curve of amino groups. **(C)** The relative amount of amino groups grafted on the PLCL membranes (**$p \leq 0.01$, ***$p \leq 0.001$).

2.6.4 Statistical analysis

The quantitative data were presented as mean ± standard error of the mean. For statistical analysis, Origin 2022 (OriginLab Corporation, Northampton, MA, United States) was used and one-way ANOVA combined with an independent sample was used to compare the significance of differences among the experimental groups. When the p-value was less than 0.05 ($p < 0.05$), the difference was considered significant.

3 Results and discussion

3.1 Preparation of biocompatible and elastic membranes

Figure 1 illustrates the procedure for the fabrication of the elastic nanofibrous PLCL membrane. PLCL co-polymer has been known as a highly biocompatible and biodegradable material and applied in several tissue engineering areas (Jeong et al., 2004; Kim et al., 2006; Yoo et al., 2021). Furthermore, it was investigated that the mechanical properties of the PLCL such as elasticity and flexibility are excellent when the ratio of LA:CL is 50:50 (Jang et al., 2012). Thus, we synthesized PLCL in the same ratio as mentioned above, and the molecular weight (M_w) and polydispersity index (PDI) of the synthesized PLCL were 121,642 g/mol and 1.95, respectively. Dissolving the PLCL in HFIP at a concentration of 10% w/v, it was confirmed that jets were formed uniformly while electrospinning. The morphological properties of nanofibers can vary depending on the electrospinning conditions, such as solvent, voltage, relative humidity (RH), and rate of drum collector (Xue et al., 2019). To specify the effect of surface modification of the PLCL fibrous membrane, all samples were electrospun in the same conditions, as mentioned in the experimental section. Especially, RH was controlled to less than 30% using a dehumidifier. As a result, the nanofibers with uniform diameters were obtained. Electrospun smooth and bead-free PLCL nanofibrous membranes were prepared, however, bare PLCL fibers are not appropriate for cell culture due to their hydrophobic natures. Therefore, they are modified using a two-step method to achieve a more

10.3389/fmats.2023.1141154

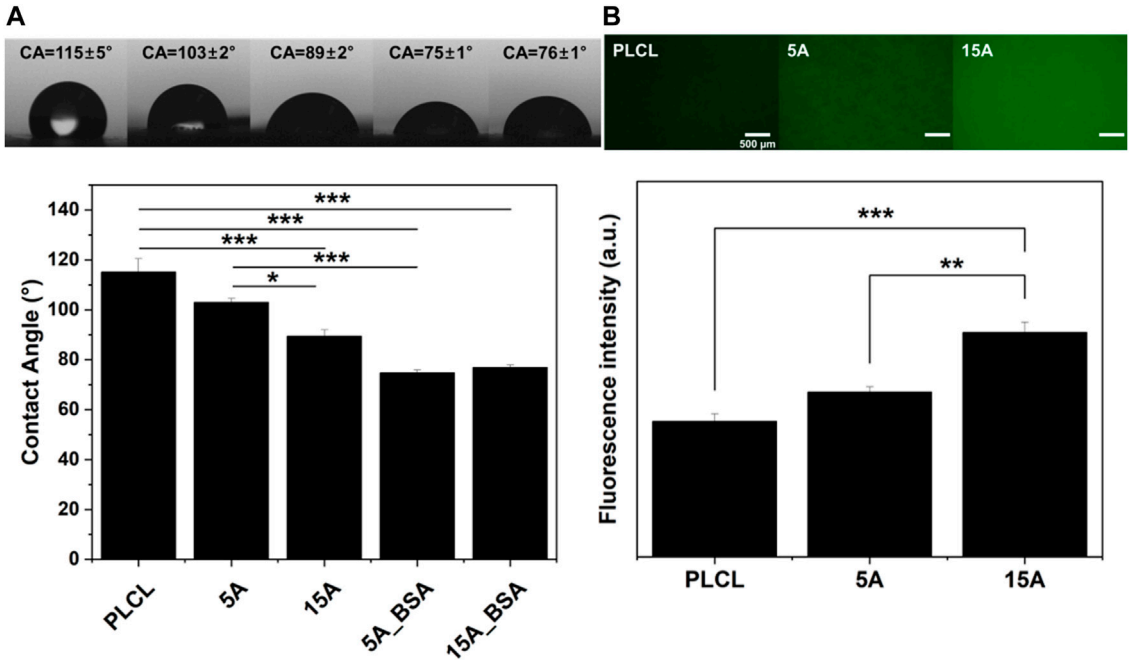

FIGURE 3
The wettability and FITC-BSA adsorption variation of the surface-modified PLCL membranes with BSA. **(A)** Water contact angle (WCA) of the PLCL membranes according to the surface modification. **(B)** Fluorescent intensities of FITC-BSA adsorption on the bare-PLCL and aminolyzed PLCL membranes. Scale bars: 500 μm (*p ≤ 0.05, **p ≤ 0.01, ***p ≤ 0.001).

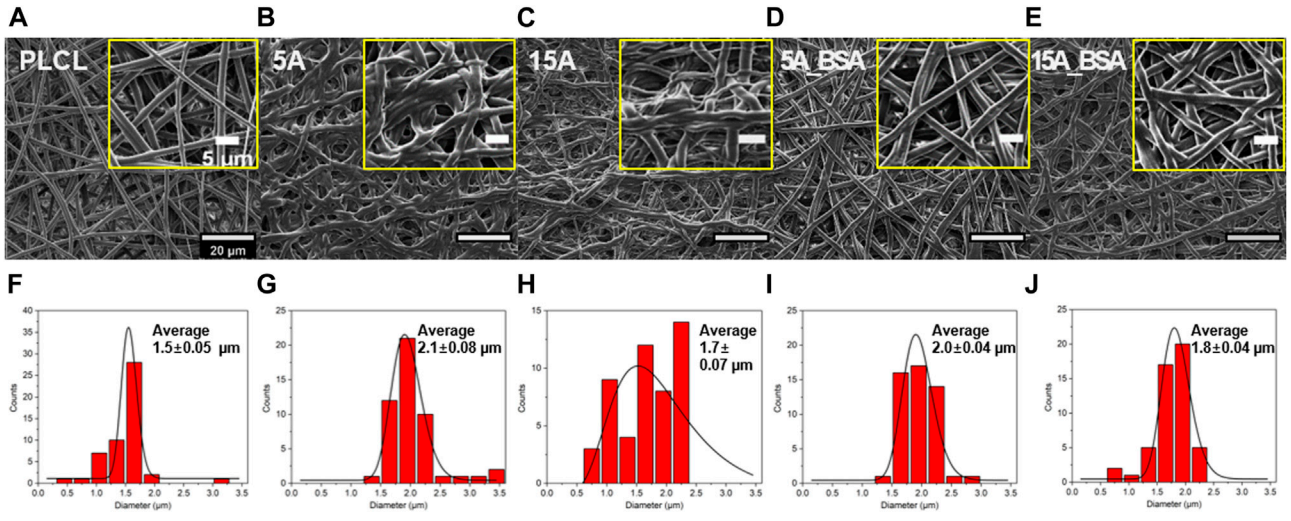

FIGURE 4
Morphological characterizations of the elastic nanofibrous PLCL membranes. **(A–G)** The scanning electron microscopy (SEM) images. **(F–J)** diameter distributions: PLCL, 5 A, 15 A, 5A_BSA, and 15A_BSA (from the left side). On the SEM images, the yellow boxes depict enlarged sections of each membrane. Scale bars: 20 μm and 5 μm.

biofunctionalized cell scaffold by altering them hydrophilic and bioactive. The first step is aminolysis using diamine and the introduction of NH_2 groups onto PLCL fibers which further help as anchoring sites for BSA on the surface and makes the surface hydrophilic.

3.2 Aminolysis of PLCL electrospun membranes

To observe the fiber morphology, roughness, and fiber quality, AFM and SEM analysis was performed for PLCL, aminolyzed PLCL

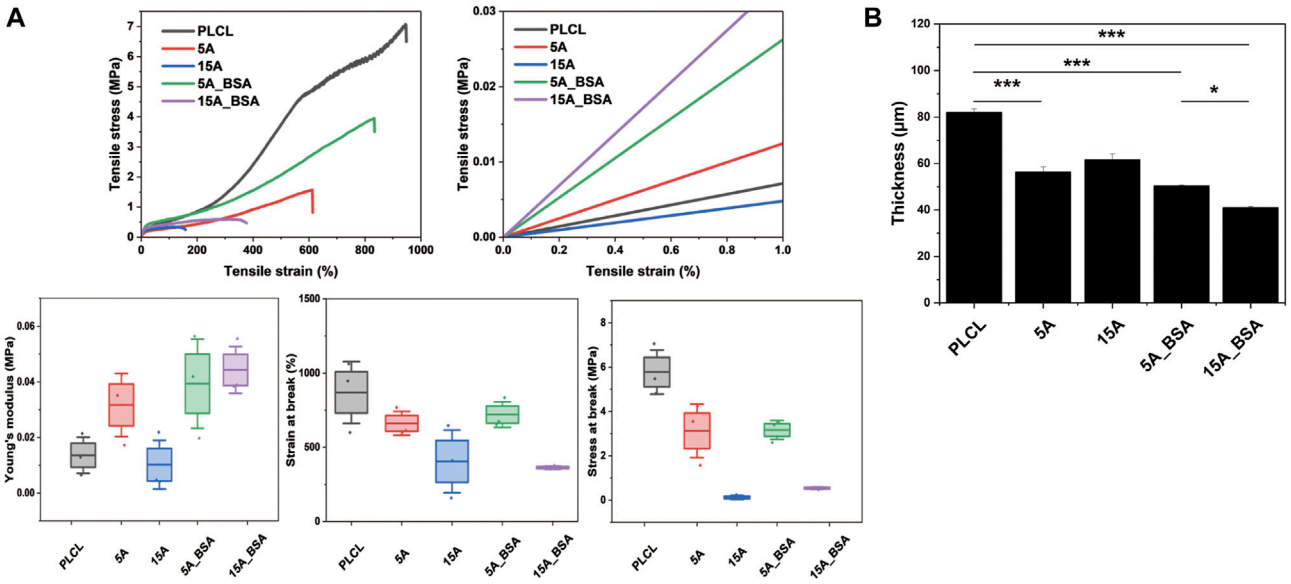

FIGURE 5
The physical properties of the bare and surface modified PLCL membranes. **(A)** Mechanical properties of the PLCL membranes; strain-stress curve, Enlarged Strain-stress curve of the left result, Young's modulus, strain at break, and stress at break. **(B)** Thickness variations of the PLCL membranes (*$p \leq 0.05$, **$p \leq 0.01$, ***$p \leq 0.001$).

(i.e., 5 A, 15 A), and BSA-immobilized PLCL (i.e., 5A_BSA, 15A_BSA) membranes. It has been observed that the aminolyzed and BSA-immobilized membranes have a similar morphology and maintain a smooth and defect-free morphology such as the PLCL membranes. Figures 2A–C shows the results of aminolysis treatment on the PLCL membranes. To confirm the presence of amine groups, ninhydrin assay was conducted. When exposed to the ninhydrin, the free amino acid undergoes oxidative deamination, finally forming diketohydrin responsible for the deep purple color (Friedman, 2004). On the basis of the ninhydrin reaction, both of the aminolyzed PLCL membranes, 5 A and 15 A, were observed to have NH_2 groups compared to the bare PLCL membrane. Specifically, 15 A changed to darker purple color than 5 A, which indicates increasing time makes more NH_2 groups grafted on the membrane as shown in Figure 2A. These results were also quantified by measuring the absorbance and calculating the concentration based on the standard curve of ethylenediamine. Figures 2B, C shows the standard curve and the relative amounts of amino groups corresponding to the bare or aminolyzed membranes. The amount of NH_2 groups of 15 A (1.05×10^{-5} M/mg) was about three times higher than those of 5 A (4.07×10^{-6} M/mg). In the EDS elemental analysis, while the N peak was detected on diamine-treated surfaces, it did not appear in the bare PLCL (Supplementary Figure S1).

3.3 Immobilization of protein on PLCL membranes

To investigate the effectiveness of aminolysis, immobilization of BSA, which promotes the cell-substrate interaction, was performed and confirmed by WCA and FITC-BSA analysis. Increasing the hydrophilicity of the surface improves cell attachment by increasing the contact area between the cell and the surface (Zhu et al., 2002; Khalili and Ahmad, 2015). Hydrophobic ester bonds of polymers can be replaced with relatively hydrophilic amide bonds *via* aminolysis, as a result, the hydrophilicity of the polymer surface increases. (Zhu et al., 2013; Taskin et al., 2021). The introduction of proteins such as BSA and RGD onto the surface also forms a hydrophilic surface by increasing the surface energy and hydrogen bonds with water molecules (Mi et al., 2018). In Figure 3A, the contact angles decreased from 115° of PLCL to 103° and 89° in the aminolyzed membranes of 5 A and 15 A, respectively. Moreover, after grafting BSA onto the surface, the values of contact angles dropped more to 75° and 76° each in 5A_BSA and 15A_BSA. These results indicate BSA was stably bound to the aminolyzed PLCL fibrous membranes. As reported in previous studies, BSA is successfully introduced onto the substrates by covalent bonding occurred between carboxyl groups (-COOH) of BSA and amino groups (-NH_2) of the surfaces. (Perelman et al., 2007; Müller et al., 2019). Based on the principle, to confirm the relative amount of BSA immobilized on the membranes, FITC-BSA was utilized. The normalized mean grey value was calculated as the intensity of fluorescence emitted from the BSA. As shown in Figure 3B, the amount of attached FITC-BSA was highest in 15 A, followed by 5 A and PLCL. Especially, 15 A indicated a significantly higher intensity of fluorescence than PLCL, meaning the increasing treatment time of aminolysis enhanced the ability of protein adsorption. Furthermore, the pre-BSA-grafted membranes (5A_BSA, 15A_BSA) had a lower amount of FITC-BSA than the bare PLCL, indicating membrane surfaces were already filled with BSA, as shown in Supplementary Figure S2. The XPS and FTIR analysis confirmed additional BSA covalent conjugation with the aminolyzed PLCL membrane. In the XPS analysis, nitrogen peaks were detected on both 5A_BSA and 15A_BSA samples. The

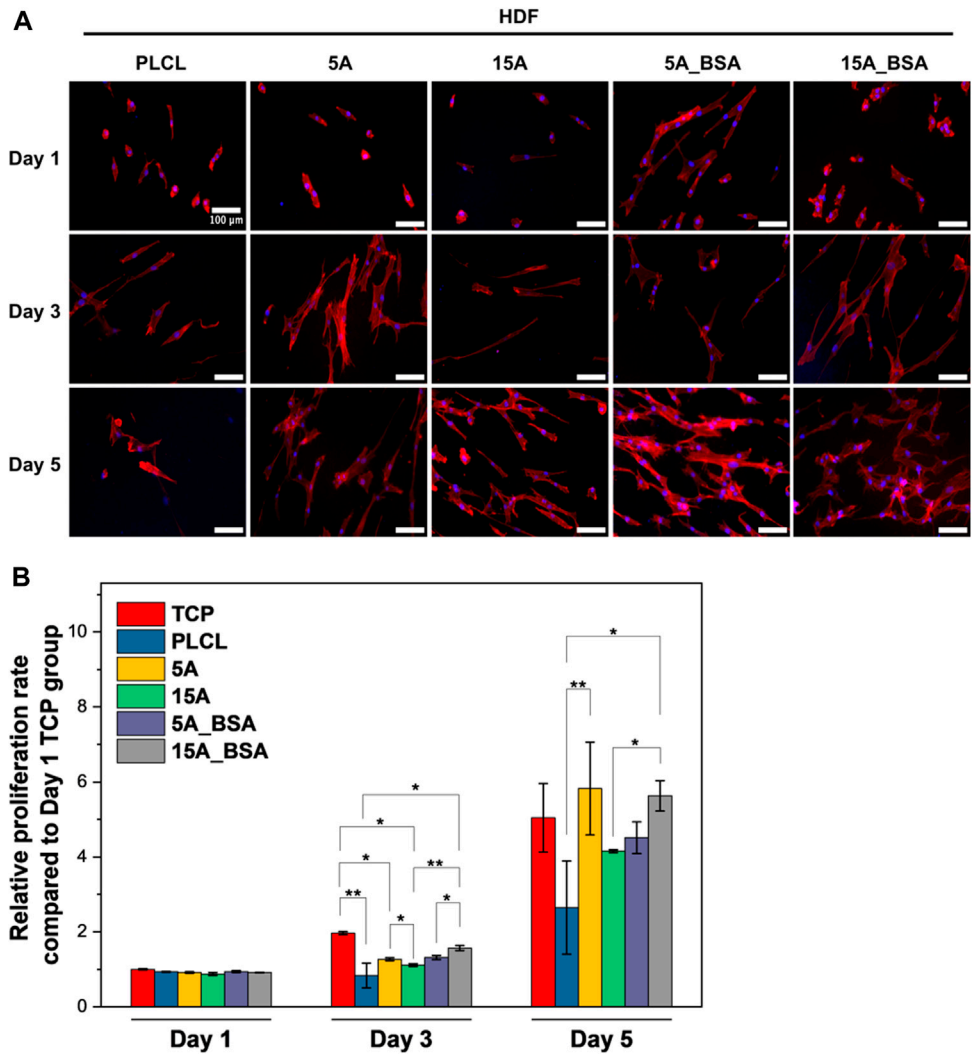

FIGURE 6
Biocompatibility of the surface modified PLCL membranes **(A)** Representative fluorescent images of stained human dermal fibroblast cells (HDFs) attached to the surface-modified PLCL membranes compared to the bare PLCL membrane (Red: F-actin and Blue: Nuclei), Scale bars: 100 μm **(B)** Cell proliferation on the surface-modified PLCL membranes compared to the bare PLCL membrane evaluated by WST-8 assay (*$p \leq 0.05$, **$p \leq 0.01$).

concentration of N on the BSA-grafted membranes was about 2 atomic % while there was no N peak on the bare PLCL membrane. In the spectrum of FTIR, there was a band of amide II at 1,470–1,570 cm^{-1} in both BSA-grafted membranes. Contrary to this, bare PLCL had no amide band, indicating the protein immobilization was successfully conducted (Supplementary Figure S3).

3.4 Physical characteristics of PLCL membranes

The morphological variations of the surface-modified PLCL membranes were analyzed by SEM images (Figure 4). From the previous studies, it was reported that chemical surface modification such as aminolysis or hydrolysis could deform the surface structure in extreme conditions, finally leading fracture of fiber (Mohabatpour et al., 2016; Jeznach et al., 2022). However, the structures of 5 A and 15 A in the SEM images were observed to be more relaxed and curled than fractured. It is presumed that the mild experimental condition (i.e., low concentration of ethylenediamine (6% w/v) and short reaction time) results in non-fractured but collapsed morphologies with increasing the averaging fiber diameter. During the aminolysis, the amorphous parts of PLCL collapsed, on the other hand, the crystalline parts kept aligned (Garkhal et al., 2007; Hetemi and Pinson, 2019; Vadas et al., 2020). These deformed parts of 5 A and 15 A were partially recovered with BSA immobilizations by the effect of a cross-linker, EDC. The roughness of the membrane dropped after the aminolysis treatment. However, as the protein was grafted, the roughness increased again at the bare PLCL level (Supplementary Figure S4).

As a factor affecting the cell behaviors, the mechanical strength of the PLCL membranes was confirmed by the uniaxial tensile test and thickness measurement. Among the five experimental groups,

the averaging tensile strength of PLCL was the strongest as stress at break and strain at break were 6 MPa and 870%, respectively (Figure 5A). In the case of the surface-modified PLCL membranes, however, the stiffness increased and the tensile strength decreased. The aminolysis cleaves the ester bond of polymeric fiber leading to a decrease of the mean molecular weight of the polymer, resulting in reduced mechanical strength (Zhu et al., 2013; Taskin et al., 2021). Interestingly, the average Young's modulus of 15A-BSA was 3 times higher than PLCL and about 4 times higher than 15 A, indicating that the immobilization process of BSA positively affected the stiffness. Notably, it was observed that the tensile strength slightly increased both in 5A_BSA and 15A_BSA compared to the aminolyzed membranes, suggesting the physical properties weakened by aminolysis could be alleviated by the protein immobilization with EDC/NHS. In effect, EDC as a cross-linker is known to directly mediate the formation of amide bonds between amino groups and carboxyl groups, as a result, polymer membranes become mechanically strong by dense molecular distances (Zhang et al., 2022). In addition, we grafted fibrinogen onto the surfaces at 200 μg/mL and observed an improvement in the tensile strength, similar to the results of BSA grafting, suggesting a generalizable effect of cross-linker EDC on mechanical properties (Supplementary Figure S7D). The Young's modulus of human skin is generally known to be 17 ± 1.6 kPa (Lorden et al., 2015), which is similar to that of the surface-modified membranes in this study. Although the tensile strength weakens in the process of surface modification, the mechanical properties are still suitable for supporting HDF cells since the stress at the break of the surface-modified membrane is higher than those of human skin (200 ± 16 kPa). It is presumed that the thickness of the aminolyzed PLCL membranes decreased (Figure 5B), which was attributed to the shrinkage behavior of the amorphous region in electrospun membranes (Fernández et al., 2012; Yuan et al., 2021). In addition, the thickness tends to decrease slightly following BSA conjugation, which can be seen as a result of EDC crosslinking.

3.5 Cell behaviors on the modified PLCL membranes

To investigate the cell affinity of the modified PLCL fibrous membranes, HDFs were cultured on each experimental membrane. The biocompatibility was then evaluated in terms of cell adhesion and cell proliferation for 5 days. As shown in Figure 6A, the cells were observed to grow on all PLCL membranes to a similar level on day 1, indicating all samples were biocompatible. However, on day 3, the cells cultured on the modified PLCL membranes exhibited more elongated shapes favorable to HDF than those on the bare PLCL membrane. More specifically, the aminolyzed membranes without BSA (5A, 15A) were observed to have a more stretched shape of cells than the bare PLCL and, on the other hand, the cells on the BSA-grafted membranes (5A_BSA, 15A_BSA) were grown to a more extensible shape than 5 A and 15 A. Between the BSA-grafted membranes, there was a difference in the degree of the cell spreading until 3 days but no outstanding differences on day 5. The proliferation of HDFs on the PLCL membranes for 5 days were shown in Figure 6B. Among the modified PLCL membranes, 15A_BSA exhibited higher proliferation of HDFs than other groups for 5 days. From the results, it is noted that BSA immobilized by amino groups (NH_2) promotes cell attachment and proliferation. A consistent tendency was observed when cell adhesive RGD peptide bound surfaces (Supplementary Figure S6). Compared to the bare PLCL, more cell spreading was observed in 5A_RGD and 15A_RGD. Especially, the morphologies of HDFs in 15A_RGD on day 5 were similar to those of cells in TCP on day 3, indicating RGD grafting plays an important role in increasing the biocompatibility of the PLCL membranes. Conclusively, the cell attachment and proliferation were improved on the BSA (or RGD) functionalized PLCL nanofibrous surfaces. In addition, we evaluated the effects of BSA solution concentration at three concentrations (20, 200, and 2000 ug/mL). After grafting BSA, we quantified the density of BSA using FITC-BSA assay and investigated the corresponding tensile properties, wettability, and cell behaviors (cell adhesion and proliferation) (Supplementary Figures S7, S8). While BSA is typically used at high concentrations as an antifouling or blocking agent (Cai et al., 2015; Lin et al., 2015), we used much lower concentration for grafting and thoroughly washed physically adsorbed BSA from the membranes. As a result, the covalently grafted BSA was able to effectively facilitate cell attachment. With the versatility of post-modification and the good biocompatibility nature of biomolecules, the PLCL electrospun membranes with desirable surface functionalities can be precisely adjusted to suit various biomedical applications.

4 Conclusion

In this study, we developed a facile method for the immobilization of BSA on elastic nanofibrous PLCL membranes by aminolysis and successive chemical functionalization. The modified PLCL membranes retain stable amino groups and BSA immobilization onto the surfaces, leading to good biocompatibility without any cellular toxicity. The BSA was grafted simply onto the hydrophobic PLCL membrane by aminolysis with EDC/NHS chemistry. Whereas the number of functional groups increases during the aminolysis treatment, the mechanical stability is reduced. However, in case proteins such as BSA were introduced onto the membranes with EDC/NHS, the mechanical strength was improved by the cross-linker of EDC, and cell attachment was also enhanced by promoting cell-surface interaction. Furthermore, the Young's modulus of the surface-modified membranes was analogous to that of human skin, which makes the environment suitable for human dermal cells to adhere. Considering the advantages of simplicity in fabrication, cytocompatibility with human skin cells, and cost-effectiveness, this surface modification method can be particularly useful in wound healing treatments. The post-spinning surface modification with aminolysis and subsequent covalent grafting of proteins can easily make the elastic nanofibrous polymer membranes cell-friendly without destroying the porous structure, suggesting a promising and facile method that could be applied in various tissue engineering fields.

Data availability statement

The raw data supporting the conclusion of this article will be made available by the authors, without undue reservation.

Author contributions

SR: Conceptualization, methodology, investigation, writing—original draft, KL: Formal analysis and investigation, YJ: Validation, formal analysis, and investigation, funding acquisition, JY: Conceptualization, data curation, supervision, writing—reviewing and editing, funding acquisition.

Funding

This work was supported by the National Research Foundation of Korea (NRF) grant funded by the Korea government (MSIT) (No. 2021RlA2C2004634) and KIST intramural grant (2E32351, 2E3232L).

Conflict of interest

The authors declare that the research was conducted in the absence of any commercial or financial relationships that could be construed as a potential conflict of interest.

Publisher's note

All claims expressed in this article are solely those of the authors and do not necessarily represent those of their affiliated organizations, or those of the publisher, the editors and the reviewers. Any product that may be evaluated in this article, or claim that may be made by its manufacturer, is not guaranteed or endorsed by the publisher.

Supplementary material

The Supplementary Material for this article can be found online at: https://www.frontiersin.org/articles/10.3389/fmats.2023.1141154/full#supplementary-material

References

Amin Yavari, S., Croes, M., Akhavan, B., Jahanmard, F., Eigenhuis, C. C., Dadbakhsh, S., et al. (2020). Layer by layer coating for bio-functionalization of additively manufactured meta-biomaterials. *Addit. Manuf.* 32, 100991. doi:10.1016/j.addma.2019.100991

Cai, B., Hu, K., Li, C., Jin, J., and Hu, Y. (2015). Bovine serum albumin bioconjugated graphene oxide: Red blood cell adhesion and hemolysis studied by QCM-D. *Appl. Surf. Sci.* 356, 844–851. doi:10.1016/j.apsusc.2015.08.178

Chung, J. J., Yoo, J., Sum, B. S. T., Li, S., Lee, S., Kim, T. H., et al. (2021). 3D printed porous methacrylate/silica hybrid scaffold for bone substitution. *Adv. Healthc. Mater* 10, e2100117. doi:10.1002/adhm.202100117

Fernández, J., Etxeberria, A., Ugartemendia, J. M., Petisco, S., and Sarasua, J. R. (2012). Effects of chain microstructures on mechanical behavior and aging of a poly(L-lactide-co-ε-caprolactone) biomedical thermoplastic-elastomer. *J. Mech. Behav. Biomed. Mater* 12, 29–38. doi:10.1016/j.jmbbm.2012.03.008

Friedman, M. (2004). Applications of the ninhydrin reaction for analysis of amino acids, peptides, and proteins to agricultural and biomedical sciences. *J. Agric. Food Chem.* 52, 385–406. doi:10.1021/jf030490p

Garkhal, K., Verma, S., Jonnalagadda, S., and Kumar, N. (2007). Fast degradable poly(L-lactide-co-ε-caprolactone) microspheres for tissue engineering: Synthesis, characterization, and degradation behavior. *J. Polym. Sci. Part A Polym. Chem.* 45, 2755–2764. doi:10.1002/pola.22031

Hetemi, D., and Pinson, J. (2019). "Functionalization of polymers by hydrolysis, aminolysis, reduction, oxidation, and some related reactions," in *Surface modification of polymers*, 211–240.

Jang, B. S., Jung, Y., Kwon, I. K., Mun, C. H., and Kim, S. H. (2012). Fibroblast culture on poly(L-lactide-co-ε-caprolactone) an electrospun nanofiber sheet. *Macromol. Res.* 20, 1234–1242. doi:10.1007/s13233-012-0180-5

Jeong, S. I., Kim, S. H., Kim, Y. H., Jung, Y., Kwon, J. H., Kim, B.-S., et al. (2004). Manufacture of elastic biodegradable PLCL scaffolds for mechano-active vascular tissue engineering. *J. Biomaterials Sci. Polym. Ed.* 15, 645–660. doi:10.1163/156856204323046906

Jeznach, O., Kolbuk, D., Marzec, M., Bernasik, A., and Sajkiewicz, P. (2022). Aminolysis as a surface functionalization method of aliphatic polyester nonwovens: Impact on material properties and biological response. *RSC Adv.* 12, 11303–11317. doi:10.1039/d2ra00542e

Jeznach, O., Kolbuk, D., and Sajkiewicz, P. (2019). Aminolysis of various aliphatic polyesters in a form of nanofibers and films. *Polym. (Basel)* 11, 1669. doi:10.3390/polym11101669

Keshvardoostchokami, M., Majidi, S. S., Huo, P., Ramachandran, R., Chen, M., and Liu, B. (2021). Electrospun nanofibers of natural and synthetic polymers as artificial extracellular matrix for tissue engineering. *Nanomaterials* 11, 21. doi:10.3390/nano11010021

Khalili, A., and Ahmad, M. (2015). A review of cell adhesion studies for biomedical and biological applications. *Int. J. Mol. Sci.* 16, 18149–18184. doi:10.3390/ijms160818149

Kim, D., Chung, J. J., Jung, Y., and Kim, S. H. (2019). The effect of Substance P/Heparin conjugated PLCL polymer coating of bioinert ePTFE vascular grafts on the recruitment of both ECs and SMCs for accelerated regeneration. *Sci. Rep.* 9, 17083. doi:10.1038/s41598-019-53514-6

Kim, S.-H., Kwon, J. H., Chung, M. S., Chung, E., Jung, Y., Kim, S. H., et al. (2006). Fabrication of a new tubular fibrous PLCL scaffold for vascular tissue engineering. *J. Biomaterials Sci. Polym. Ed.* 17, 1359–1374. doi:10.1163/156856206778937244

Lin, J., Zhou, W., Han, S., Bunpetch, V., Zhao, K., Liu, C., et al. (2018). Cell-material interactions in tendon tissue engineering. *Acta Biomater.* 70, 1–11. doi:10.1016/j.actbio.2018.01.012

Lin, Y., Liu, K., Wang, C., Li, L., and Liu, Y. (2015). Electrochemical immunosensor for detection of epidermal growth factor reaching lower detection limit: Toward oxidized glutathione as a more efficient blocking reagent for the antibody functionalized silver nanoparticles and antigen interaction. *Anal. Chem.* 87, 8047–8051. doi:10.1021/acs.analchem.5b01834

Lorden, E. R., Miller, K. J., Bashirov, L., Ibrahim, M. M., Hammett, E., Jung, Y., et al. (2015). Mitigation of hypertrophic scar contraction via an elastomeric biodegradable scaffold. *Biomaterials* 43, 61–70. doi:10.1016/j.biomaterials.2014.12.003

Ma, Z., Mao, Z., and Gao, C. (2007). Surface modification and property analysis of biomedical polymers used for tissue engineering. *Colloids Surf. B Biointerfaces* 60, 137–157. doi:10.1016/j.colsurfb.2007.06.019

Masaeli, E., Karamali, F., Loghmani, S., Eslaminejad, M. B., and Nasr-Esfahani, M. H. (2017). Bio-engineered electrospun nanofibrous membranes using cartilage extracellular matrix particles. *J. Mater. Chem. B* 5, 765–776. doi:10.1039/c6tb02015a

Mi, H.-Y., Jing, X., Thomsom, J. A., and Turng, L.-S. (2018). Promoting endothelial cell affinity and antithrombogenicity of polytetrafluoroethylene (PTFE) by mussel-inspired modification and RGD/heparin grafting. *J. Mater. Chem. B* 6, 3475–3485. doi:10.1039/c8tb00654g

Mohabatpour, F., Karkhaneh, A., and Sharifi, A. M. (2016). A hydrogel/fiber composite scaffold for chondrocyte encapsulation in cartilage tissue regeneration. *RSC Adv.* 6, 83135–83145. doi:10.1039/c6ra15592h

Morelli, A., and Hawker, M. J. (2021). Utilizing radio frequency plasma treatment to modify polymeric materials for biomedical applications. *ACS Biomater. Sci. Eng.* 2021, 0c01673. doi:10.1021/acsbiomaterials.0c01673

Müller, A., Langó, T., Turiák, L., Ãcs, A., Várady, G., Kucsma, N., et al. (2019). Covalently modified carboxyl side chains on cell surface leads to a novel method toward topology analysis of transmembrane proteins. *Sci. Rep.* 9, 15729. doi:10.1038/s41598-019-52188-4

Oktay, B., Demir, S., and Kayaman-Apohan, N. (2015). Immobilization of alpha-amylase onto poly(glycidyl methacrylate) grafted electrospun fibers by ATRP. *Mater Sci. Eng. C Mater Biol. Appl.* 50, 386–393. doi:10.1016/j.msec.2015.02.033

Perelman, L. A., Schwartz, M. P., Wohlrab, A. M., Vannieuwenhze, M. S., and Sailor, M. J. (2007). A simplified biomolecule attachment strategy for biosensing using a porous Si oxide interferometer. *Phys. status solidi (a)* 204, 1394–1398. doi:10.1002/pssa.200674360

Powell, H. M., and Boyce, S. T. (2006). EDC cross-linking improves skin substitute strength and stability. *Biomaterials* 27, 5821–5827. doi:10.1016/j.biomaterials.2006.07.030

Psarra, E., König, U., Müller, M., Bittrich, E., Eichhorn, K.-J., Welzel, P. B., et al. (2017). *In situ* monitoring of linear RGD-peptide bioconjugation with nanoscale polymer brushes. *ACS Omega* 2, 946–958. doi:10.1021/acsomega.6b00450

Schmidt, M., Abdul Latif, A., Prager, A., Glaser, R., and Schulze, A. (2021). Highly efficient one-step protein immobilization on polymer membranes supported by response surface methodology. *Front. Chem.* 9, 804698. doi:10.3389/fchem.2021.804698

Smith, S., Goodge, K., Delaney, M., Struzyk, A., Tansey, N., and Frey, M. (2020). A comprehensive review of the covalent immobilization of biomolecules onto electrospun nanofibers. *Nanomater. (Basel)* 10, 2142. doi:10.3390/nano10112142

Taskin, M. B., Ahmad, T., Wistlich, L., Meinel, L., Schmitz, M., Rossi, A., et al. (2021). Bioactive electrospun fibers: Fabrication strategies and a critical review of surface-sensitive characterization and quantification. *Chem. Rev.* 121, 11194–11237. doi:10.1021/acs.chemrev.0c00816

Teo, A. J. T., Mishra, A., Park, I., Kim, Y.-J., Park, W.-T., and Yoon, Y.-J. (2016). Polymeric biomaterials for medical implants and Devices. *ACS Biomaterials Sci. Eng.* 2, 454–472. doi:10.1021/acsbiomaterials.5b00429

Vadas, D., Nagy, Z. K., Csontos, I., Marosi, G., and Bocz, K. (2020). Effects of thermal annealing and solvent-induced crystallization on the structure and properties of poly(lactic acid) microfibres produced by high-speed electrospinning. *J. Therm. Analysis Calorim.* 142, 581–594. doi:10.1007/s10973-019-09191-8

Xue, J., Wu, T., Dai, Y., and Xia, Y. (2019). Electrospinning and electrospun nanofibers: Methods, materials, and applications. *Chem. Rev.* 119, 5298–5415. doi:10.1021/acs.chemrev.8b00593

Yan, B., Zhang, Y., Li, Z., Zhou, P., and Mao, Y. (2022). Electrospun nanofibrous membrane for biomedical application. *SN Appl. Sci.* 4, 172. doi:10.1007/s42452-022-05056-2

Yao, T., Baker, M. B., and Moroni, L. (2020). Strategies to improve nanofibrous scaffolds for vascular tissue engineering. *Nanomaterials* 10, 887. doi:10.3390/nano10050887

Yoo, J., Kim, T. H., Park, S., Char, K., Kim, S. H., Chung, J. J., et al. (2021). Use of elastic, porous, and ultrathin Co-culture membranes to control the endothelial barrier function via cell alignment. *Adv. Funct. Mater.* 31, 2008172. doi:10.1002/adfm.202008172

Yoo, J., Park, J. H., Kwon, Y. W., Chung, J. J., Choi, I. C., Nam, J. J., et al. (2020). Augmented peripheral nerve regeneration through elastic nerve guidance conduits prepared using a porous PLCL membrane with a 3D printed collagen hydrogel. *Biomaterials Sci.* 8, 6261–6271. doi:10.1039/d0bm00847h

Yuan, C., Jin, S., Wei, J., Huang, J., Liu, C., Lei, X., et al. (2021). The shrinking behavior, mechanism and anti-shrinkage resolution of an electrospun PLGA membrane. *J. Mater. Chem. B* 9, 5861–5868. doi:10.1039/d1tb00734c

Zhang, L., Li, Y., and Jiang, W. (2022). A novel wound dressing material for full-thickness skin defects composed of a crosslinked acellular swim bladder. *Front. Mater.* 9. doi:10.3389/fmats.2022.1037386

Zhu, Y., Gao, C., Liu, X., and Shen, J. (2002). Surface modification of polycaprolactone membrane via aminolysis and biomacromolecule immobilization for promoting cytocompatibility of human endothelial cells. *Biomacromolecules* 3, 1312–1319. doi:10.1021/bm020074y

Zhu, Y., Mao, Z., and Gao, C. (2013). Aminolysis-based surface modification of polyesters for biomedical applications. *RSC Adv.* 3, 2509–2519. doi:10.1039/c2ra22358a